The Kinetics of Oxidation of Molybdenite Concentrate by Water Vapor

EDGAR BLANCO, HONG YONG SOHN, GILSOO HAN, and KLIMENT Y. HAKOBYAN

A thermodynamic and kinetics investigation on the oxidation of MoS_2 in molybdenite concentrate to MoO_2 by water vapor was carried out as part of new process development. The kinetics of the reaction were determined by measuring the weight change of a sample with time in water vapor at temperatures between 700 °C and 1000 °C. The reaction rate followed the shrinking-unreacted-core model under chemical reaction control, which showed activation energy of 102 kJ/mol. In addition, the behavior of rhenium and selenium in molybdenum concentrate during the process was investigated. While most rhenium remained with the molybdenum dioxide during the water vapor oxidation, almost all selenium was volatilized in agreement with thermodynamic analysis.

DOI: 10.1007/s11663-006-9001-6

I. INTRODUCTION

MOLYBDENITE (MoS_2) is the major mineral for molybdenum. In the conventional pyrometallurgical process, oxidation roasting is applied to produce MoO_3, one of the commercial products containing Mo. However, there are several serious problems in processing molybdenite by this method: Valuable elements in the concentrate such as rhenium and selenium cannot be recovered easily to high degrees and air pollution may occur due to the emission of SO_2 gas.[1,2] The rhenium-bearing off-gas is scrubbed and the scrubbing solution is subjected to ion exchange to recover part of the rhenium contained in the concentrate. However, this process is expensive and has poor recovery efficiency.

Sohn[3–6] and Hakobyan[7] investigated a water-vapor oxidation process as an alternative to the conventional roasting process. This new process offers the possibility of lower emission of sulfur containing pollutants by recovering the sulfur in MoS_2 in an elemental form. It also makes it easier to extract valuable minor elements from the ore.

The major objective of this research was to study the feasibility of this new process and to determine the kinetics of oxidation of MoS_2 by water vapor.

EDGAR BLANCO, Graduate Student, HONG YONG SOHN, Professor, and GILSOO HAN, Postdoctoral Fellow, are with the Department of Metallurgical Engineering, University of Utah, Salt Lake City, UT 84112. Contact e-mail: hysohn@mines.utah.edu KLIMENT Y. HAKOBYAN, Head and Principal Investigator, is with the, Navro Ltd., Kapan, Armenia 377810, and the Kapan Metallurgy and Enrichment Laboratory, Academy of Science of Armenia, Kapan Town, Armenia, 377810.

Manuscript submitted April 19, 2006.
Article published online July 10, 2007.

II. EXPERIMENTAL

The experimental setup used in this study is shown in Figure 1. It consisted of a water-vapor feeding system with an evaporator, a movable vertical tube furnace with vertical trail, a reactor, and an off-gas system with a NaOH-solution scrubber. The reactor had a double wall: the outer wall was a stainless steel tube and the inner wall was a mullite tube with 45-mm inner diameter, which prevented hydrogen generation from the reaction between water vapor and stainless steel at high temperatures.

The sample used in this study was a molybdenite concentrate containing 80 pct MoS_2 screened to – 60 mesh size. Figure 2 shows the size distribution of the sample measured using a Beckman Coulter laser diffraction analyzer model LS230 (Beckman Coulter, Inc., Fullerton, CA). This figure also shows the size distribution of the oxidation products to be discussed subsequently. The chemical composition of the concentrate is summarized in Table I. The sample was homogenized and kept in a desiccator after being dried to remove moisture and a small amount of oil used for flotation.

A layer of sample powder with a thickness of 1 mm was placed in an alumina tray and put into the vertical reactor. The reactor, purged with Ar gas, was positioned in the furnace by pulling up the furnace after the temperature of the furnace reached the desired temperature. Then, the Ar purging was stopped after the temperature of the sample was brought to the desired value, and liquid water was injected into the reactor for a predetermined length of time. All the water is evaporated in the top part of the reactor to 86.7 kPa pressure, the atmospheric pressure at Salt Lake City. The weight change during the reaction was measured from the weights of the solid sample before and after the reaction. Chemical analysis and microstructure

observation were performed using X-ray diffraction (XRD), inductively coupled plasma (ICP), and scanning electron microscopy (SEM).

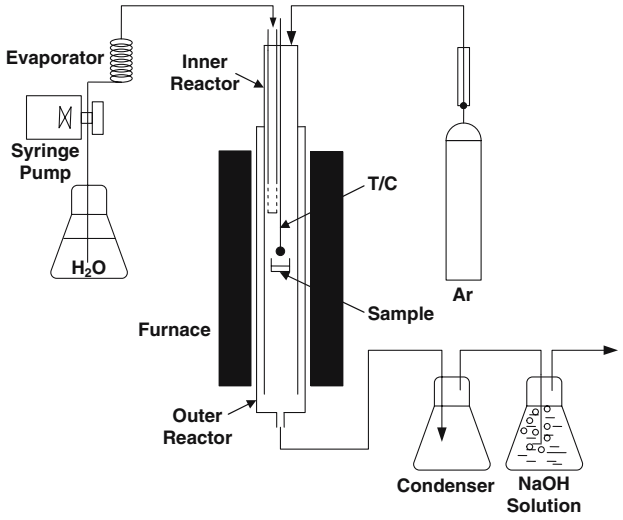

Fig. 1—Experimental apparatus.

	D_{50}(μm)	D_{80}(μm)
MoS_2	116.4	213.2
MoO_2	111.0	177.0

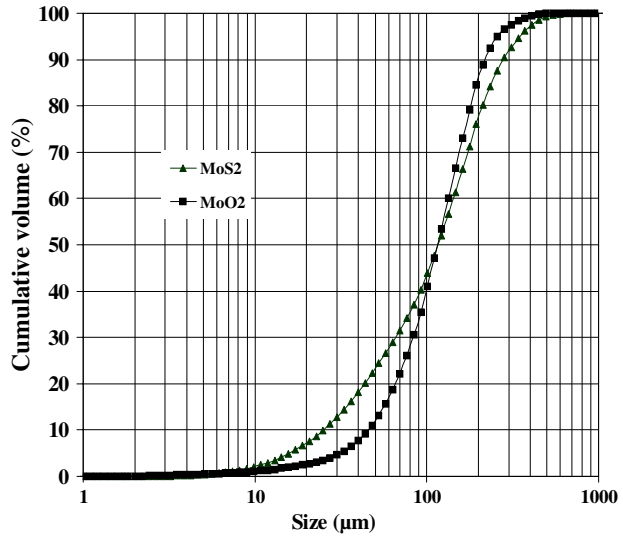

Fig. 2—Particle size distribution of molybdenite concentrate and the oxidation product MoO_2.

III. RESULTS AND DISCUSSION

A. *Thermodynamics*

The equilibrium compositions in the MoS_2-H_2O (g) system at various temperatures were calculated using HSC Chemistry software developed by Outokumpu Research Oy, which is based on the principle of Gibbs free energy minimization. Figure 3 shows the equilibrium amounts of the major species present when 1 mol of MoS_2 is reacted with 100 mol of H_2O (g). It is seen that the main solid product at high temperatures is MoO_2 rather than MoO_3, which is the stable phase in a conventional roasting process using oxygen gas, and that the gaseous product is a mixture of H_2 (g), H_2S (g), and SO_2 (g). Thus, the reaction between MoS_2 and H_2O can be represented by

$$MoS_2 + xH_2O\ (g) = MoO_2 + yH_2\ (g) + zH_2S\ (g) + wSO_2\ (g) \quad [1]$$

the ratios among the gaseous products determined by thermodynamics at equilibrium and also by kinetics in general. According to this analysis, there is a possibility that elemental sulfur can be recovered from the off-gas by the Claus process and that hydrogen can be recovered as a byproduct. A detailed analysis including the amounts of gaseous products was beyond the scope of this work.

To predict the behavior of Re and Se in the MoS_2 concentrate, the equilibrium compositions of Re and Se compounds in 1 mol MoS_2-100 mol H_2O (g)-0.001 mol ReS_2-0.001 mol Se were calculated, as shown

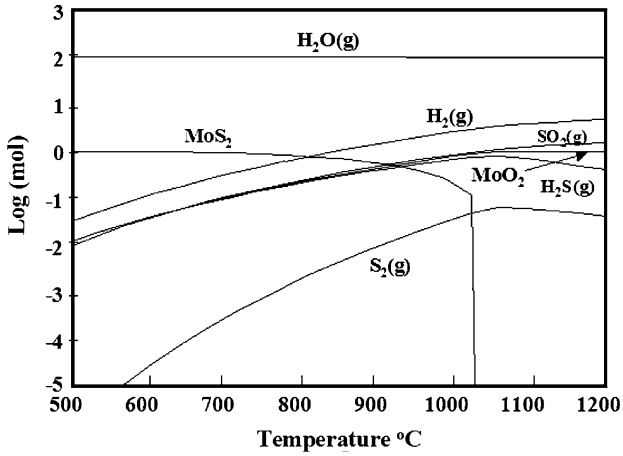

Fig. 3—Equilibrium composition *vs* temperature for a mixture of 1 mol MoS_2-100 mol H_2O.

Table I. Chemical Composition of the Molybdenite Concentrate

Element	Mo	S	SiO_2	CaO	Al_2O_3	MgO	Na + K	Cu	Zn
Wt pct	47.1	36.5	5.03	1.20	0.45	0.30	0.29	0.67	0.03
Element	Ni	Co	Mn	Fe	As	H_2O + Oil	Se	Re	Te
Wt pct	0.16	0.06	0.04	1.8	0.03	6.2	236 ppm	264 ppm	86 ppm

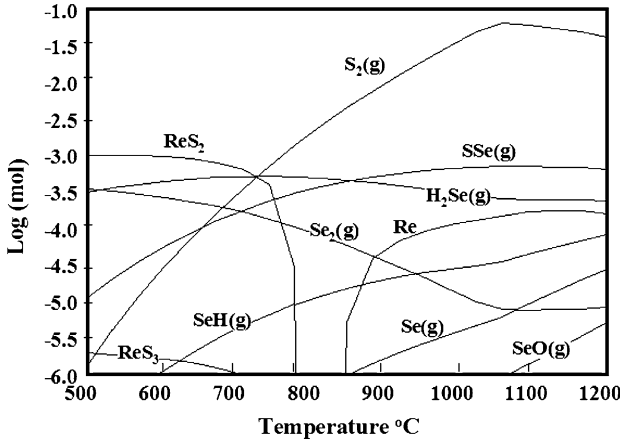

Fig. 4—Equilibrium composition of Re and Se compounds against temperature for a mixture of 1 mol MoS_2-100 mol H_2O-0.001 mol ReS_2-0.001 mol Se.

in Figure 4. While the stable Re phases are elemental Re at high temperatures and ReS_2 at low temperatures, those of Se are gaseous phases such as SeS (g), SeH (g), and Se_2 (g). Thus, it is expected that Re will remain in solid products after the water vapor oxidation and that Se should be collected from the off-gas system. (The result in Figure 4 shows just the lower part of the overall equilibrium calculation. Because of the low concentrations of the species shown in this part in the presence of the dominant species consisting of Mo, H, S, and O, the amounts shown here contain some round-off errors exemplified by the absence of any rhenium between 800 °C and 855 °C.)

B. *Kinetics of Oxidation of Molybdenite by Water Vapor*

Kinetic experiments were conducted by measuring the weight change of a sample with time in an environment containing 100 pct water vapor. The weight change during the reaction was measured from the weights of the solid sample before and after each run. Continuous weight measurement was difficult in this work for various reasons including the problem of vaporizing water without generating a pressure pulse. Pulsed water vapor flow is no problem in a batch run made in the absence of mass-transfer effects. It is important in determining the reaction rate of individual concentrate particles to eliminate the effect of external mass transfer between the bulk gas and particle surface as well as the effect of interparticle diffusion. Thus, the experiments were performed to determine the minimum water feeding rate above which a further increase does not affect the reaction rate, thus indicating the elimination of external mass-transfer effect. The interparticle diffusional effect was eliminated by using a shallow layer of particles, as mentioned previously. Figure 5 shows the results for five different water feeding rates at 1000 °C using approximately 300-mg samples. As the water feeding rate increased, the conversion rate increased due to the mass-transfer effects. However, the rate for 4 mL/min was essentially the same as that for 6 mL/min, which

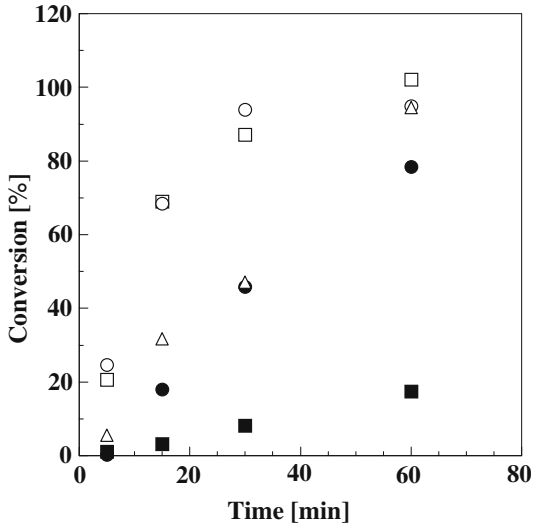

Fig. 5—Conversion *vs* reaction time at 1000 °C for five different liquid water feeding rates: ○ 6 mL/min, □ 4 mL/min, Δ 2 mL/min, • 1 mL/min, and ■ 0.1 mL/min (300 mg samples). All the water is evaporated in the top part of the reactor to 86.7 kPa pressure, the atmospheric pressure at Salt Lake City.

indicated that above 4 mL/min of water feeding rate, the mass transfer is sufficiently fast and thus does not affect the reaction rate. Based on this result, the feeding rate of 4 mL/min was applied to other experiments. The product of these experiments was MoO_2, as shown in Figure 6, which is consistent with the thermodynamic analysis. The size distribution of the MoO_2 particles thus produced is shown in Figure 2.

The effect of reaction temperature on the overall reaction rate was investigated with the water feeding rate of 4 mL/min and at six different temperatures. The weights of the samples were all approximately 300 mg except for the cases of 120-min reaction time in which approximately 800-mg samples were used. It was determined that the sample amount (even a 2-g sample) did not affect the conversion *vs* time relationship in the

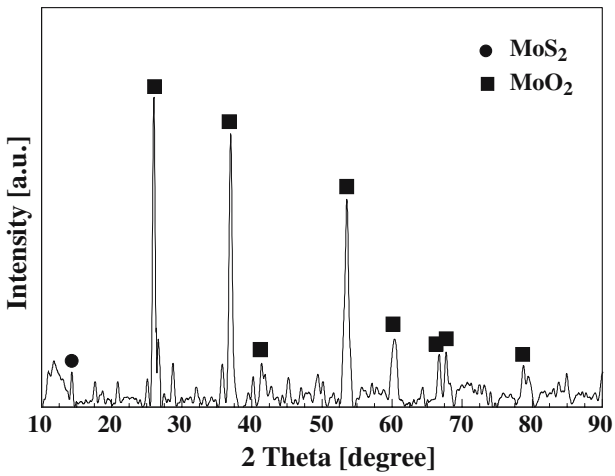

Fig. 6—XRD pattern for the sample after a 2-h experiment at 1000 °C at the water feeding rate of 1 mL/min.

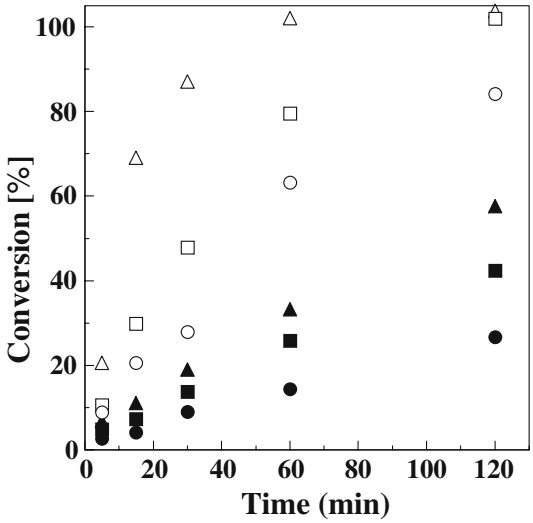

Fig. 7—Conversion *vs* reaction time at the liquid water feeding rate of 4 mL/min for six different temperatures: • 700 °C, ■ 800 °C, ▲ 850 °C, ○ 900 °C, □ 950 °C, and △ 1000 °C. (All the water is evaporated in the top part of the reactor to 86.7 kPa pressure, the atmospheric pressure at Salt Lake City.

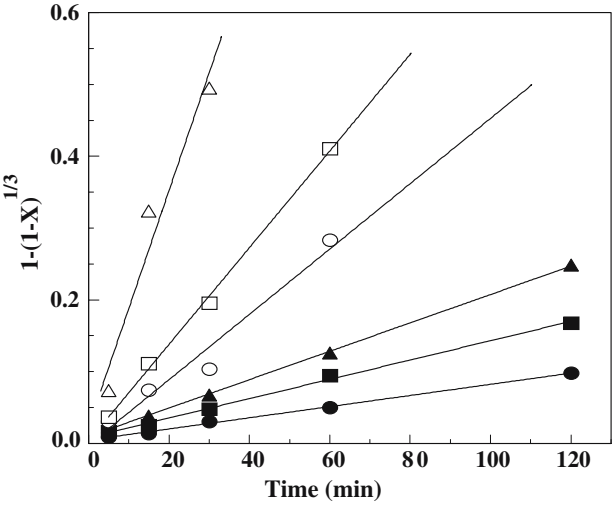

Fig. 9—Conversion-time curves prepared from Fig. 7 according to Eq. [1]: • 700 °C, ■ 800 °C, ▲ 850 °C, ○ 900 °C, □ 950 °C, and △ 1000 °C.

range tested. This condition must be met when the objective is to determine the kinetics unaffected by interstitial diffusion and external mass transfer. The results are shown in Figure 7 for the temperature range 700 °C to 1000 °C. As expected, the conversion rate increased with temperature. These results were applied to a shrinking-unreacted-core rate model.[8] This rate expression relates the conversion to the reaction time by

$$k_{\text{app}} \cdot t = 1 - (1 - X)^{1/F_p} \qquad [2]$$

where k_{app} is the apparent rate constant, t is the reaction time, X is the conversion, and F_p is the shape factor whose value is 1, 2, and 3, respectively, for flat plates, long cylinders, and spheres (or equidimensional in all directions). To determine the shape factor, the morphologies of MoS_2 and MoO_2 were investigated by the use of SEM, as shown in Figure 8, which indicated that the shape was almost equidimensional in all directions. Thus, the value of 3 was chosen as the shape factor for these samples. The conversion data in Figure 7 were plotted according to Eq. [2] in Figure 9, which shows a straight line at each temperature. (The three highest conversion values were calculated to be slightly greater than 100 pct, because of small uncertainties in experimental measurements. Such points cannot be displayed in Figure 8 due to the nature of the vertical scale.) This rate equation was further verified after trying a number of different rate models such as the shrinking-core model with different shape factors and the nucleation-and-growth model. The values of k_{app} were obtained from the slopes of the straight lines in Figure 9 and were subjected to an Arrhenius plot yielding an activation energy value of 102.4 kJ/mol, as shown in Figure 10.

C. *Behavior of Rhenium and Selenium*

To determine the behavior of rhenium and selenium, their concentrations relative to Mo in the MoS_2 concentrate and MoO_2 samples produced from it were measured by ICP. The MoO_2 samples were prepared under the condition of 950 °C reaction temperature,

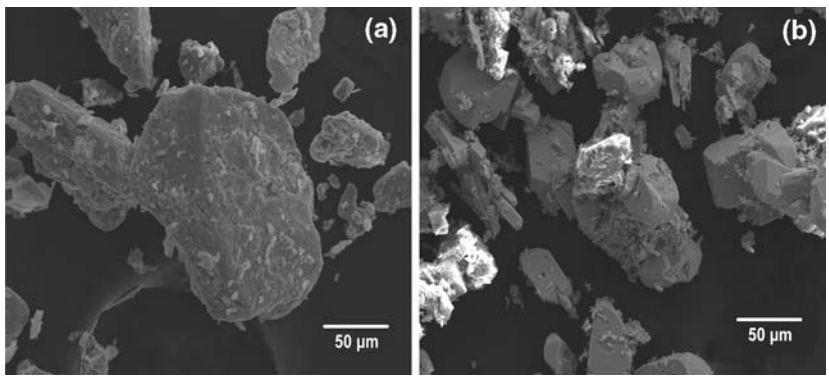

Fig. 8—SEM pictures of (*a*) MoS_2 concentrate and (*b*) MoO_2 produced after the experiments.

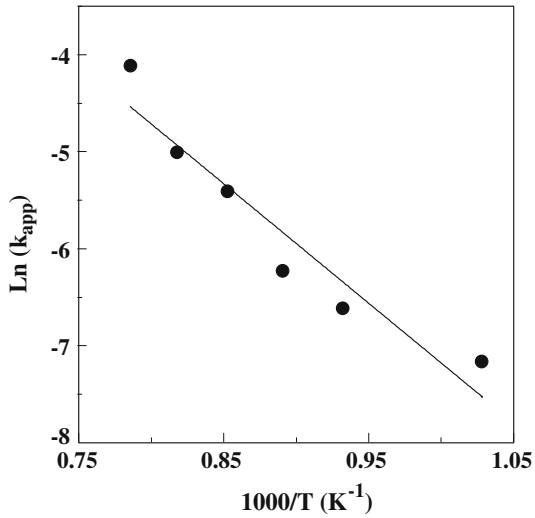

Fig. 10—Arrhenius plot of apparent rate constants k_{app} for the reaction of MoS_2 with water vapor.

Table II. Mo, Re, and Se Concentrations before and after the Water-Vapor Oxidation of the Concentrate

Sample	Mo (Wt Pct)	Re (ppm)	Se (ppm)	Re/Mo	Se/Mo
MoS_2 Conc.	48.3	264	236	5.47×10^{-4}	4.88×10^{-4}
MoO_2	55.7	270	0	4.85×10^{-4}	0

3.5 hours of reaction time, and 4 mL/min of water feeding rate to obtain essentially 100 pct conversion. While most of the rhenium remained in the MoO_2 sample after the water vapor oxidation, almost all of the selenium disappeared from the sample, as shown in Table II. These experimental results agreed well with the thermodynamic analysis, that is, Re remained in the MoO_2 product as a solid compound and Se was evaporated as gaseous compounds from the solid sample. Thus, Re can be extracted from this solid product without a serious loss during the oxidation process and Se can be extracted from the off-gas scrubber.

D. *Treatment of the Sulfur-Containing Off-Gas*

The equilibrium off-gas from the oxidation of MoS_2 with water vapor contains H_2S and SO_2, as can be seen in Figure 3. When the gas is separated from the solid and cooled, the ratio of H_2S and SO_2 contents becomes higher, which was confirmed by thermodynamic calculations.[9] These gases can then be converted to elemental sulfur by the following Claus reaction:

$$2H_2S + SO_2 = 3S + 2H_2O \quad [3]$$

A more detailed description of this topic in conjunction with the development of a process based on the treatment of molybdenite concentrates is the topic of another article.[9]

IV. CONCLUSIONS

The product of water-vapor oxidation of molybdenum sulfide at high temperature was MoO_2, which is consistent with the thermodynamic analyses. Kinetic analyses showed that the shrinking-unreacted-core model under chemical reaction control was applicable to the reaction of molybdenum sulfide with water vapor at high temperatures. This reaction had an activation energy of 102.4 kJ/mol. Rhenium in the molybdenum sulfide concentrate remained in the solid product, and selenium was evaporated as gaseous selenium compounds.

ACKNOWLEDGMENT

This work was supported by the United States Civilian Research and Development Foundation under Project No. AE2-2526-KA-03.

REFERENCES

1. C.K. Gupta: *Extractive Metallurgy of Molybdenum*, CRC Press, Inc., Boca Raton, FL, 1992, pp. 67–72.
2. D. Kim: Ph.D. Thesis, University of Utah, Salt Lake City, UT, 1980.
3. H.Y. Sohn: U.S. Patent No. 4,376,647, Mar. 15, 1983.
4. H.Y. Sohn and D. Kim: *J. Met.*, 1984, vol. 36 (1), pp. 67–73.
5. H.Y. Sohn and D. Kim: *Metall. Trans. B*, 1987, vol. 18B, pp. 451–57.
6. H.Y. Sohn and D. Kim: *Metall. Trans. B*, 1988, vol. 19B, pp. 973–75.
7. K. Hakobyan and A. Hakobyan: Eurasia Patent No. 002417, Aug. 12, 1998.
8. J. Szekely, J.W. Evans, and H.Y. Sohn: *Gas-Solid Reactions*, Academic Press, Inc., New York, 1976, pp. 73–89.
9. K.Y. Hakobyan, H.Y. Sohn, A.K. Hakobyan, V.A. Bryukvin, V.G. Leontiev, and O.I. Tsibin: *Trans. Inst. Mining Metall., Sec. C*, in press.